Hybrid Simulated Annealing for Multi–Objective Capacitated Vehicle Routing in School Milk Distribution

Peerapong Pakawanich*

Department of Industrial Engineering and Management, Faculty of Engineering and Industrial Technology, Silpakorn University Sanam Chandra Palace Campus, Phra Prathom Chedi, Mueang, Nakhon Pathom, 73000, Thailand

***Corresponding Author E–mail:** pakawanich_p@su.ac.th.

Received: Oct 01, 2025; **Revised:** Dec 02, 2025; **Accepted:** Dec 11, 2025

Abstract

This study develops a Hybrid Multi–Objective Simulated Annealing (HMOSA) framework for solving the Multi–Objective Capacitated Vehicle Routing Problem in Thailand's School Milk Program, where balancing efficiency and fairness is essential due to the manual unloading tasks performed by each delivery team. The model minimizes total travel distance and workload imbalance, quantified by the standard deviation of vehicle loads to better capture physical handling effort. The proposed HMOSA introduces two novel mechanisms: i) warm–start initialization using extreme seed solutions generated from Single–Objective SA (SOSA) and Weighted–Sum SA (WSSA), and ii) a guided neighborhood mechanism that selects promising neighbors using weighted scores to enhance search efficiency and diversity. These contributions improve convergence stability without relying on complex parameter tuning. Computational experiments on 10, 30, and 51–customer instances demonstrate that HMOSA consistently outperforms conventional MOSA and SA, and provides superior Pareto–front quality compared with Non-dominated Sorting Genetic Algorithm II NSGA–II. Performance was assessed using two widely adopted indicators: hypervolume (HV) for solution diversity and inverted generational distance (IGD) for convergence reliability. In the real–world 51–school case, small increases in total distance resulted in substantial improvements in workload equity, offering actionable compromise solutions between distance and fairness. Overall, HMOSA embeds fairness into routing decisions while maintaining scalability and robustness, serving as a practical decision–support tool for real routing applications where routing efficiency and equitable workload distribution are both essential.

Keywords: Capacitated vehicle routing problem, Hybrid simulated annealing, workload balance, Multi–objective

1. Introduction

Transportation and logistics services play a vital role in ensuring the smooth flow of goods across supply chains and enabling economic activities across regions. Efficient distribution planning is essential for minimizing delays, reducing transportation costs, and maintaining service reliability. However, real–world logistics operations often involve complexities such as limited vehicle capacities, irregular demand patterns, uncertain traffic conditions, and manual loading and unloading tasks. These factors frequently lead to planning difficulties, operational inefficiencies, and excessive workload on certain delivery teams, highlighting the need for operationally viable routing strategies that can support practical decision–making in logistics operations.

To tackle these logistics challenges, a wide range of metaheuristic algorithms have been employed. Population–based approaches such as Genetic Algorithms [1–5], Particle Swarm Optimization [6] and Ant Colony Optimization [7] have been successfully applied to various routing scenarios. However, these methods often require complex parameter tuning and large population management. In contrast, Simulated Annealing (SA) provides a simpler yet flexible single–solution framework and has demonstrated strong performance across multiple VRP variants [8–11].

Within the research community, the Vehicle Routing Problem (VRP) provides the primary modeling framework for studying distribution challenges. Classical VRP models focus on minimizing total transportation cost [1],[4],[12], while more recent studies incorporate broader objectives related to environmental sustainability, service quality, and operational reliability [13–18]. These developments demonstrate a growing interest in multi–objective routing models that better reflect practical logistics requirements.

Workload balancing across delivery routes has gained increasing attention in vehicle routing studies [19], with various approaches proposed to reflect fairness and efficiency in distribution operations. Lehuédé et al. [20] introduced a lexicographic minimax approach for route balancing in the VRP. Unlike traditional min–max methods, their model sought to progressively equalize route durations in descending order, thereby avoiding inconsistencies and promoting a fairer workload distribution among drivers. Shahnejat–Bushehri et al. [21] addressed workload balancing in the context of healthcare logistics during the COVID–19 pandemic. Their model defined workload in terms of total working time, including travel and service duration, and aimed to fairly assign routes to testers. Using a mixed–integer programming model and adaptive large neighborhood search (ALNS), they achieved significantly better outcomes than real–world operations. Li et al. [22] proposed a cluster–based optimization framework for the VRP with workload balance (VRPWB), where workload was defined as

the combination of travel distance and delivery volume. Their multi–phase solution, using micro cluster fusion and a modified ant colony optimization (ACO) algorithm, proved effective in both first–mile and last–mile logistics settings. In 2025, Zhao et al. [23] presented a bi–objective urban logistics VRP model that jointly optimized total delivery cost and route workload to improve both operational efficiency and employee satisfaction. Workload was represented using route duration, and the proposed hybrid metaheuristic (MDLS with path relinking) effectively balanced operational and social objectives. Most recently, Xu and Ouyang [24] studied physical load balance in pallet–based logistics through the 2L–SDVRPTW–LB model. Their focus was on achieving axle weight balance across semi–trailer trucks to ensure vehicle stability and road safety. A branch–and–cut algorithm was used to handle this complex problem, reflecting concerns unique to large–volume or palletized logistics systems.

Prior research often approximated workload using route distance or the number of serviced customers, while some studies have adopted total working time that includes travel, waiting, and service durations to better reflect operational effort under time window constraints [23]. However, these approaches mainly capture time–related dimensions and may not fully represent the physical burden in logistics environments where manual handling is dominant. This limitation becomes particularly evident in real distribution settings, such as the Thai School Milk Program.

In the distribution of school milk, for example, delivery teams are responsible not only for transportation but also for lifting and unloading a substantial volume of milk pouches at each school. Under such labor–intensive conditions, time–based metrics alone may not accurately quantify human workload. A related study by Li et al. [22] combined both travel distance and delivery load into a single workload index and balanced it using a ratio–based objective. While this formulation captures overall operational effort, the aggregation of travel and manual handling into one measure may dilute the relative impact of physical labor in contexts where human effort is a critical concern. Therefore, in the present study, workload is represented solely by the total carried load, and the imbalance across routes is minimized to more directly reflect physical effort and promote fairness in real delivery operations. Based on this motivation, the school milk distribution problem is formulated as a Multi–Objective Capacitated Vehicle Routing Problem (MO–CVRP) that simultaneously minimizes travel distance and workload imbalance across delivery routes.

To support informed decision–making in real logistics environments, a Hybrid Multi–Objective Simulated Annealing (HMOSA) algorithm is proposed. A key aspect of the method is the use of structured warm–start initialization. Instead of relying on random solutions, HMOSA adapts Single–Objective SA (SOSA) and Weighted–Sum SA (WSSA) to generate extreme seed solutions for both objectives. This design serves two practical purposes. First, it accelerates early convergence and reduces sensitivity to parameter settings. Second, and more importantly from a managerial standpoint, extreme solutions allow decision–makers to explicitly observe how total distance increases when workload balance is introduced as an additional objective. In typical routing practices where only distance minimization is considered, such trade–offs are rarely visualized or evaluated. The use of extreme seed solutions therefore enables planners to understand the consequences of balancing fairness with total distance and select routing strategies aligned with operational priorities.

Furthermore, a fixed–probability acceptance rule is incorporated to preserve diversity among mutually non–dominated neighbors. Conventional adaptive probability schemes may increase computational burden or require calibration that varies across problem instances, which introduces additional learning time before consistent solutions can be obtained. The fixed strategy proposed in this study provides a more practical alternative by eliminating the need for probability learning during runtime and enabling faster convergence toward diverse non–dominated solutions. Such responsiveness is important in real–world applications, where practitioners typically require decision support that delivers solutions quickly and consistently without extensive parameter tuning.

Finally, standard deviation of vehicle loads is adopted as the second objective. This metric was chosen because it provides a clear and interpretable indication of workload imbalance that can be directly communicated to decision–makers. When multiple routes must be discussed with stakeholders, a transparent measure of variation supports more effective evaluation and justification of alternative routing plans.

In this way, the proposed framework functions as a managerial decision–support tool that enables the comparison of routing scenarios under competing objectives. It guides planners in assessing when an improvement in fairness may justify a modest increase in total travel distance, thereby making the trade–off between routing efficiency and equitable task allocation explicit and actionable.

2. Problem Statement

The problem under consideration is a variant of the CVRP. A single depot is responsible for serving a set of customer nodes with known demands. A homogeneous fleet of vehicles, each with limited capacity, is available to perform the deliveries. Each vehicle must start and end its route at the depot, and each customer must be visited exactly once by a single vehicle.

In the real distribution system of the School Milk Program, deliveries follow a daily cycle: refrigerated trucks are loaded at a central depot each morning, visit all assigned schools, and return after completing their

routes. No intermediate reloading or split delivery is allowed, and there are no strict time windows since all routes are typically completed within regular working hours. Each vehicle is staffed by a driver and a delivery assistant, who must manually unload all milk pouches at every school. These operational characteristics justify modeling the distribution task as a capacitated VRP while also considering workload fairness, as manual handling effort is directly related to the carried load. A detailed description of the numerical data is presented in the experimental section.

Two conflicting objectives are considered. The first is to minimize the total travel distance of all vehicles. The second is to minimize the imbalance of vehicle workloads, measured by the standard deviation of vehicle loads, in order to ensure fairness among delivery teams. This formulation is referred to as a MO–CVRP.

Based on this problem description, the MO–CVRP can be mathematically formulated as follows.

2.1 Mathematical Formulation

Indices and sets

i index of origin nodes, $\boldsymbol{I} = \{0, 1, 2, \ldots, n\}$

j index of destination nodes, $\boldsymbol{J} = \{0, 1, 2, \ldots, n\}$ where $j \neq i$.

k index of vehicles, $\boldsymbol{K} = \{1, 2, \ldots, K\}$

$\boldsymbol{A}$ set of directed arcs between nodes, $\boldsymbol{A} = \{(i, j) \; i \in \boldsymbol{I}, j \in \boldsymbol{J}, i \neq j\}$

Input parameters

D_j demand at customer node j

Q vehicle capacity

C_{ij} travel distance from node i to node j

Decision variable

x_{ijk} = 1 if vehicle k travel from node i to node j, 0 otherwise.

Objective functions

Minimize total distance

$$\text{Min } z_1 = \sum_{i \in \boldsymbol{I}} \sum_{j \in \boldsymbol{J}} \sum_{k \in \boldsymbol{K}} C_{ij} x_{ijk} \tag{1}$$

Eq. (1) seeks to minimize the total distance traveled by all vehicles.

Minimize the standard deviation of vehicle loads

$$\text{Min } z_2 = \sqrt{\frac{1}{|\boldsymbol{K}|} \sum_{k \in \boldsymbol{K}} (L_k - \bar{L})^2} \tag{2}$$

where $L_k = \sum_{i \in \boldsymbol{I}} \sum_{j \in \boldsymbol{J},\, j \neq 0} D_j x_{ijk}$, $\forall k \in \boldsymbol{K}$ represents the total load assigned to vehicle k. The average L_k ($\bar{L}$) is computed from $\bar{L} = \sum_{k \in \boldsymbol{K}} \frac{L_k}{|\boldsymbol{K}|}$ and $|\boldsymbol{K}|$ is the cardinality of set $\boldsymbol{K}$.

Eq. (2) minimizes the standard deviation of vehicle loads, thereby promoting balanced utilization of the fleet.

Constraints

Each customer is entered exactly once (across the fleet)

$$\sum_{i \in \boldsymbol{I}} \sum_{k \in \boldsymbol{K}} x_{ijk} = 1, \quad \forall j \in \boldsymbol{J} \backslash \{0\} \tag{3}$$

Eq. (3) guarantees that each customer j (excluding the depot) is served exactly once by one vehicle, ensuring complete and non–redundant coverage of demand points.

Flow conservation

$$\sum_{i \in \boldsymbol{I}} x_{ijk} = \sum_{i \in \boldsymbol{I}} x_{jik}, \forall j \in \boldsymbol{J}, \forall k \in \boldsymbol{K} \tag{4}$$

Eq. (4) enforces flow conservation at each customer node. For every vehicle k, the number of arcs entering a customer node j must equal the number of arcs leaving it, thereby maintaining route continuity.

Each vehicle must depart from the depot at the start of its route.

$$\sum_{j \in \boldsymbol{J},\, j \neq 0} x_{0jk} = 1, \quad \forall k \in \boldsymbol{K} \tag{5}$$

Eq. (5) ensures that each vehicle departs from the depot exactly once, establishing the starting point of every route.

Vehicle load capacity

$$\sum_{i \in \boldsymbol{I}} \sum_{j \in \boldsymbol{J},\, j \neq 0} D_j x_{ijk} \leq Q, \quad \forall k \in \boldsymbol{K} \tag{6}$$

Eq. (6) restricts the total assigned load of vehicle k not to exceed its maximum capacity Q. This reflects real–world resource limitations and ensures feasibility of the delivery plan.

Binary constraint

Eq. (7) indicates that x_{ijk} is binary.

$$x_{ijk} \in \{0, 1\}, \forall i \in \boldsymbol{I}, \; \forall j \in \boldsymbol{J}, \; \forall k \in \boldsymbol{K} \tag{7}$$

In classical CVRP formulations, subtour elimination constraints are often included to explicitly prevent the formation of disconnected cycles. In this study, such constraints are not incorporated in the mathematical model. Instead, feasibility is ensured through the design of the HMOSA algorithm, where candidate solutions are represented as complete vehicle routes starting and ending at the depot. The neighborhood operators (Swap, Insert, Reverse), together with the repair mechanism, inherently generate feasible routes without subtours. As a result, the algorithm is capable of producing valid solutions while avoiding the additional computational burden of subtour elimination constraints.

3. Methodology

This study proposes a Hybrid Multi–Objective Simulated Annealing (HMOSA) to solve a Multi–Objective CVRP (MO–CVRP) that minimizes both the total travel distance and the load imbalance among vehicles. The method extends the conventional MOSA by introducing two key components: (i) a warm–start strategy using extreme seed solutions generated from single–objective simulated annealing (SOSA) and weighted–sum simulated annealing (WSSA), and (ii) a guided neighborhood mechanism that selects the most promising neighbor among multiple candidates based on a normalized weighted score. HMOSA preserves Pareto–based acceptance and maintains an external archive of non–dominated solutions.

3.1 Inputs

The algorithm requires a distance matrix, customer demands, and vehicle capacities. Simulated annealing parameters are the initial temperature $T_{initial}$, the minimum temperature T_{min}, the cooling rate α, and the number of iterations per temperature level. HMOSA parameters include the maximum archive size and the probability $p_{accept\_nondominated}$ for accepting mutually non–dominated neighbors. Guidance parameters are the probability p_{guided_use}, the number of candidate neighbors $k_{candidates}$, and a discrete set of weights.

3.2 Solution representation and feasibility

A solution is encoded as a set of routes assigned to vehicles, where each route begins and ends at the depot. Feasibility requires that every customer is visited exactly once and that the vehicle load does not exceed its capacity. When any constraint is violated, a repair operator relocates customers to restore feasibility.

In classical CVRP formulations, subtour elimination constraints are typically included to prevent disconnected cycles. In the proposed approach, such constraints are not added to the mathematical model because feasibility is maintained directly by the algorithmic structure of HMOSA. All candidate solutions are encoded as full depot–to–depot routes, and new solutions are generated using Swap, Insert and Reverse operators that operate only on feasible routes. As a result, fragmented tours do not occur during the search process.

If any violation occurs, such as excess load or loss of route continuity, the repair mechanism immediately adjusts the solution. Furthermore, only feasible solutions are retained in the archive, ensuring that all stored solutions remain valid. In this way, subtours are inherently avoided without requiring additional constraints, which reduces computational effort while preserving feasibility at every iteration.

3.3 Objectives and dominance

Each solution S is evaluated by two objectives: $f(S)=(d(S), \sigma(S))$, where $d(S)$ is the total travel distance and $\sigma(S)$ is the standard deviation of route loads. Dominance follows the Pareto minimization rule: solution x dominates solution y if it is no worse in both objectives and strictly better in at least one objective.

3.4 Warm–start with extreme seeds.

The algorithm first generates a set of extreme seed solutions by running SOSA separately for distance and load imbalance, and WSSA for weight w=1.0 (distance only) and w=0.0 (load imbalance only). These seeds represent different search directions and are inserted into the external archive to provide diverse starting points for exploration. The initial solution for MOSA is then selected from the seed set using a balanced weighted score with w=0.5, which helps initiate the search from a reasonable compromise between distance and workload balance.

This strategy avoids starting from a purely random solution and reduces the risk of premature convergence by allowing the algorithm to explore both extreme ends of the objective spectrum from the beginning. As a result, the search process is accelerated while maintaining diversity, which improves the overall convergence behavior of HMOSA.

3.5 Guided neighborhood mechanism.

At each iteration, with probability p_{guided_use}, guided search is performed. A weight is drawn from the weights set, and up to $k_{candidates}$ feasible neighbors are generated using Swap, Insert, or Reverse operators. The neighbor with the lowest normalized weighted score is selected. Distances and load imbalances are normalized by ranges estimated from sampled feasible solutions. This mechanism acts as a soft directional guide that improves exploitation without fully abandoning random exploration. By occasionally prioritizing neighbors with better weighted scores, HMOSA can focus the search toward promising regions of the Pareto front while still preserving diversity. This balance helps reduce random walk behavior and supports stable convergence toward well–distributed non–dominated solutions.

3.6 Acceptance rules and archive update.

Acceptance is determined by three cases: (i) a dominating neighbor is always accepted, (ii) a dominated neighbor is accepted with probability $\exp(-loss/T)$, where the loss is the normalized deterioration in objectives, and (iii) non–dominated neighbors are accepted with probability $p_{accept\_nondominated}$. Each accepted solution is added to the archive, which retains only non–dominated solutions and truncates to the maximum size if necessary.

3.7 Cooling schedule and termination.

The temperature decreases geometrically as $T \leftarrow \alpha \times T$. The algorithm terminates when $T \leq T_{min}$, and the final archive is returned as the set of non–dominated solutions.

Based on the aforementioned design, the complete algorithmic flow of HMOSA is summarized in the pseudocode shown in **Figure 1**.

To provide a standard evolutionary benchmark, the Non–dominated Sorting Genetic Algorithm II (NSGA–II) was implemented using a permutation–based representation, where each chromosome encodes vehicle routes that start and end at the depot while satisfying capacity constraints. Binary tournament selection was employed, and offspring were generated using order crossover (OX) and swap mutation adapted to the CVRP

route structure. NSGA–II follows the classical process of combining parent and offspring populations, sorting them into non–dominated fronts, and preserving diversity via crowding distance. The method is included solely as a baseline to benchmark the proposed HMOSA framework under comparable computational effort.

Hybrid Multi–Objective Simulated Annealing (HMOSA)
Input:
Distance matrix, customer demands, vehicle capacities; SA parameters: $T_{initial}$, T_{min}, α (cooling rate), iterations_per_T
HMOSA parameters: archive_max_size, $p_{accept\_nondominated}$
Hybrid guidance parameters: p_{guided_use}, $k_{candidates}$, weights_set; Neighborhood operators: Swap, Insert, Reverse
Procedure HMOSA():
// Step 1: Initialization with Warm–Start
Generate a set of extreme seed solutions S_{seeds} by running SOSA (for min distance and min sd) and WSSA (for w=0 and w=1).
Initialize a feasible solution $S_{current}$ from S_{seeds}.
Initialize Archive A with all solutions from S_{seeds}.
$T \leftarrow T_{initial}$
// Step 2: Main Simulated Annealing Loop
while $T > T_{min}$ do
for iter = 1 to iterations_per_T do
// Step 3: Hybrid Neighborhood Search
if random() < p_{guided_use} then
// Guided search: generate k candidates and select the one with the best weighted score.
Select a random weight w from weights_set.
Generate a pool of $k_{candidates}$ S_c from $S_{current}$ using random operators.
$S_{neighbor} \leftarrow$ argmin(S_c, weighted score(w))
else
// Standard random search: generate one neighbor.
$S_{neighbor} \leftarrow$ apply random operator ($S_{current}$)
// Ensure the neighbor is feasible.
Repair $S_{neighbor}$ if infeasible
// Step 4: Multi–Objective Acceptance Criteria
Evaluate objectives f($S_{neighbor}$) = (TotalDistance, LoadSTD).
if f($S_{neighbor}$) dominates f($S_{current}$) then
$S_{current} \leftarrow S_{neighbor}$
else if f($S_{current}$) dominates f($S_{neighbor}$) then
Calculate loss based on the normalized deterioration in objectives.
if random() < exp(–*loss* / T) then
$S_{current} \leftarrow S_{neighbor}$
else
// Both solutions are non–dominated.
if random() < $p_{accept\_nondominated}$ then
$S_{current} \leftarrow S_{neighbor}$
// Step 5: Update Archive and Temperature
Update Archive A with $S_{neighbor}$ if it is a non–dominated solution.
end for
$T \leftarrow T * \alpha$
end while
return the set of non–dominated solutions from Archive A

Figure 1 Pseudocode of the proposed HMOSA algorithm

In addition to the metaheuristic baseline, an exact method was included to provide a reference for solution optimality. A simplified branch and bound (B&B) procedure was developed for the 10–customer pilot instance. The method was adapted specifically for the MO–CVRP by constructing routes sequentially for multiple vehicles, enforcing capacity feasibility during branching, and closing each route by returning to the depot before starting the next one. A cost–based bound was applied to prune partial solutions whose accumulated travel cost already exceeded the best complete solution found so far. Although this B&B variant does not incorporate load balancing, it offers an exact reference

for routing distance and serves as the benchmark for evaluating solution quality in the pilot test.

4. Numerical example

To demonstrate the applicability of the proposed MO–CVRP model and the HMOSA solution approach, a numerical example is conducted based on the school milk distribution problem. The example illustrates how the model can be instantiated with real operational data and how the algorithm performs in generating efficient and balanced delivery routes.

4.1 Case Description

This study is motivated by Thailand's School Milk Program, a long–standing national initiative to promote children's nutrition. In this program, pasteurized milk is transported daily from a central depot to designated schools within each region. The case investigated here involves a contractor responsible for distributing milk to 51 schools and one depot, making a total of 52 delivery points. The fleet consists of eight refrigerated trucks, each with a capacity of 3,500 pouches (pch.), giving an overall delivery capacity of 28,000 pch.. Daily school demands vary considerably, ranging from 120 to 1,247 pch., with a total demand of 25,157 pch.

Operational details add further complexity beyond routing. Each vehicle is manned by a driver and a delivery assistant, who are jointly responsible not only for transporting milk but also for unloading and physically delivering pouches to each school. Consequently, if a vehicle is assigned to schools with consistently higher demand, the delivery team faces disproportionately heavier manual workloads compared to other teams. This highlights the importance of balancing workloads in addition to minimizing travel distances. Although time windows are common in many VRP variations, they were not treated as binding constraints in this case study. In the real operation of the School Milk Program, milk is delivered using refrigerated vehicles, and all routes can be completed within the normal daily distribution period without approaching any critical time limit. Therefore, no strict delivery–time windows or maximum route duration are enforced by the distributor. The geographic distribution of the depot and schools is illustrated in **Figure 2**.

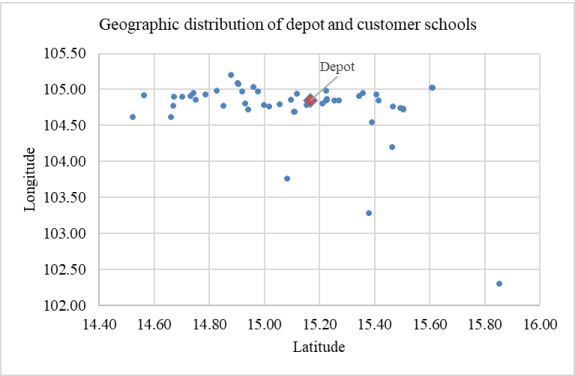

Figure 2. Geographic distribution of the depot and school customers in the study area

Based on the geographic coordinates illustrated in **Figure 2**, the distance matrix was constructed by applying the Haversine formula to compute the great–circle distance between every pair of nodes. This approach provides a realistic approximation of travel distances from latitude and longitude values without requiring detailed road network data.

4.2 Parameter Settings

The HMOSA algorithm requires parameters related to simulated annealing as well as the multi–objective search. To account for differences in problem scale, three configurations were adopted: a pilot test with 10 customers, an intermediate case with 30 customers, and the main case study with 51 customers. **Table 1** summarizes the settings.

Table 1 Parameter settings for pilot and main case study

Parameter	Number of Customers		
	10	**30**	**51**
T_0	100	300	500
T_{min}	10^{-3}	10^{-3}	10^{-3}
Cooling rate	0.990	0.993	0.995
Iterations per temperature	10	15	20
Archive size	100	250	400
$p_{accept\_nondominated}$	0.9	0.9	0.9
Number of runs	10	10	10

The smaller 10–customer instance was used as a pilot test to validate HMOSA against an exact algorithm (branch–and–bound). Accordingly, lighter settings were employed, such as a lower initial temperature and faster cooling rate, to reduce computational effort while still enabling meaningful exploration. The 30–customer case served as a transitional benchmark, for which moderately increased parameters were used to strike a balance between computational tractability and the need for a broader search space. For the 51–customer case study, more extensive settings were required to cope with the larger search space. A higher initial temperature and slower cooling schedule allowed broader exploration, while a larger archive size preserved the diversity of Pareto–approximated solutions. Across all three scales, the acceptance probability for non–dominated solutions was kept constant at 0.9 to maintain a consistent trade–off between exploration and exploitation. In addition, the probability of using guided search was fixed at 0.50, which provided a moderate level of direction without reducing search diversity.

To enable a fair and competitive comparison, the NSGA–II was implemented as an evolutionary benchmark baseline. Although it is not the focus of this study, its parameters were chosen to match the computational effort of HMOSA. For each problem size, a fixed population size and generation limit were used: (pop = 40, gen = 120) for 10 customers, (pop =

60, gen = 350) for 30 customers, and (pop = 80, gen = 650) for 51 customers. Binary tournament selection was adopted, and offspring were generated using order crossover (OX) and swap mutation, with crossover and mutation probabilities fixed at 0.9 and 0.2, respectively. All runs were executed ten times, as in HMOSA. These settings are commonly used in multi–objective VRP studies and allow NSGA–II to remain competitive as a baseline, while HMOSA incorporates additional mechanisms to explicitly enhance diversity and guided local search.

The algorithm was implemented in Python and executed on a desktop equipped with an Intel(R) Core(TM) i7–4720HQ CPU running at 2.60 GHz and 8 GB of RAM. For each problem size, the algorithm was run independently ten times to account for the stochastic nature of the search process.

5. Results and Discussion

5.1 Computational Results and Performance Assessment

This section presents the computational results of the proposed HMOSA. The algorithm was first validated on a small 10–customer instance using an exact algorithm (B&B) as a reference, before being applied to the 51–customer school milk distribution case. Each algorithm was executed independently 10 times to account for stochastic variability, and the results are analyzed in terms of both solution quality and consistency. The performance comparison is shown in **Table 2**.

Table 2 Performance comparison of B&B, SA, MOSA, NSGA–II and HMOSA on small case

	BD (km.)	BLSD (pch.)	Avg. BD (km.)	Avg. BLSD (pch.)	Time (sec)
B&B	149.67	–	149.67	–	2.06
SA	149.67	2.50	149.67	3.00	0.67
MOSA	149.67	2.50	154.99	2.50	0.96
NSGA–II	149.67	102.50	149.67	102.50	0.75
HMOSA	149.67	2.50	153.66	2.50	2.28

Note: B&B = branch and bound; SA = simulated annealing; MOSA = multi–objective simulated annealing; NSGA–II = non–dominated sorting genetic algorithm II; HMOSA = hybrid multi–objective simulated annealing. BD = Best distance; BLSD = Best load standard deviation; "Avg." = reports the mean over 10 independent runs. km. = kilometer and pch. = pouches.

From **Table 2**, the exact algorithm (B&B) achieved the shortest routing distance of 149.67 km, which serves as the reference optimum for the small–scale instance. Although it does not address load balancing, it provides a useful benchmark for evaluating optimality gaps.

SA matched this best distance and improved load balance with a best standard deviation of 2.50 pch. Its performance was also highly stable, with an average distance of 149.67 km and an average load SD of 3.00 pch., corresponding to 0.00% optimality gap relative to B&B.

MOSA also reached the same best total distance, and its average distance of 154.99 km yielded an optimality gap of 3.56%, indicating a moderate deterioration in travel distance when compared with the reference solution.

In contrast, NSGA–II, while achieving the same best distance, exhibited a significantly higher load imbalance of 102.50 pch. In terms of routing efficiency, its average distance resulted in an optimality gap of 0.00%, but its high variability in load indicates that further mechanisms are required to enhance workload fairness within population–based approaches.

The proposed HMOSA achieved an average distance of 153.66 km, corresponding to an optimality gap of 2.66%, while maintaining the same best load standard deviation of 2.50 pch. This represents a notable improvement over MOSA, both in terms of solution stability and load balancing.

Overall, these results confirm that HMOSA achieves a balanced trade–off between routing efficiency and workload fairness. With a lower optimality gap than MOSA and a vastly smaller load imbalance than NSGA–II, HMOSA demonstrates strong convergence properties and improved practical relevance. The next section expands the analysis to an intermediate 30–customer case to examine scalability before proceeding to the real–world 51–customer distribution problem.

Table 3 presents the results of the intermediate 30–customer instance. Unlike the previous small case, this scenario involves greater routing complexity, leading to a wider performance gap among the algorithms. SA continued to provide a competitive routing solution with the lowest best distance of 648.61 km. and a best load SD of 0.49 pch., although its average distance increased to 664.14 km. MOSA, on the other hand, showed a notable deterioration in both distance and workload balance, with an average distance of 875.26 km. and a high average load SD of 8.54 pch.

Table 3 Performance comparison of B&B, SA, MOSA, NSGA–II and HMOSA on intermediate case

	BD (km.)	BLSD (pch.)	Avg. BD (km.)	Avg. BLSD (pch.)	Time (sec)
SA	648.61	0.49	664.14	1.93	2.01
MOSA	842.97	4.76	875.26	8.54	2.52
NSGA–II	732.79	5.00	766.75	5.79	4.43
HMOSA	648.77	1.65	648.77	1.02	7.59

Note: B&B = branch and bound; SA = simulated annealing; MOSA = multi–objective simulated annealing; NSGA–II = non–dominated sorting genetic algorithm II; HMOSA = hybrid multi–objective simulated annealing. BD = Best distance; BLSD = Best load standard deviation; "Avg." = reports the mean over 10 independent runs. km. = kilometer and pch. = pouches.

NSGA–II achieved a moderate routing distance and demonstrated reasonable consistency; however, its best and average load SD values remained higher than those of SA and HMOSA, which implies that while NSGA–II can maintain competitive routing performance, achieving adequate workload fairness may require additional balancing mechanisms.

The proposed HMOSA obtained a balanced performance across objectives. It achieved a best distance of 648.77 km. that was comparable to SA, while reducing the average load SD to 1.02 pch., yielding the lowest variability among all methods. These observations indicate that HMOSA preserved solution quality and stability when the problem scale increased, suggesting that its search mechanism can adapt effectively to larger routing instances. The next section applies the algorithm to the real–world 51–customer distribution case to assess its practical deployment potential. This reinforces the role of structured warm–start and archive–guided acceptance in sustaining performance under increased problem complexity.

Table 4 presents the computational results for the real–world school milk distribution case. SA yielded relatively short routes, with a best distance of 1,348.67 km. and an average distance of 1,369.67 km. It also produced low load variability (best = 1.57 pch., average = 1.93 pch.), demonstrating strong performance in the single–objective setting. However, SA does not generate a set of non–dominated solutions, which may limit practical decision–making when trade–offs between objectives must be considered.

Table 4 Performance comparison of B&B, SA, MOSA, NSGA–II and HMOSA on the real–world case study

	BD (km.)	**BLSD (pch.)**	**Avg. BD (km.)**	**Avg. BLSD (pch.)**	**Time (sec)**
SA	1,348.67	1.57	1,369.67	1.93	5.53
MOSA	2,308.40	36.75	2,357.20	45.61	7.25
NSGA–II	1,706.80	5.15	1,797.33	9.09	15.27
HMOSA	1,346.85	1.65	1,346.85	1.65	21.03

Note: B&B = branch and bound; SA = simulated annealing; MOSA = multi–objective simulated annealing; NSGA–II = non–dominated sorting genetic algorithm II; HMOSA = hybrid multi–objective simulated annealing. BD = Best distance; BLSD = Best load standard deviation; "Avg." = reports the mean over 10 independent runs. km. = kilometer and pch. = pouches.

MOSA generated a more diverse solution set but tended to converge to regions with considerably higher distances, with a best of 2,308.40 km. and an average of 2,357.20 km. The workload imbalance was also significantly higher (best load SD = 36.75 pch., average = 45.61 pch.), indicating that it struggled to maintain consistent trade–offs between route efficiency and workload balance.

NSGA–II provided a more balanced performance compared with MOSA, achieving a best routing distance of 1,706.80 km. and a best load SD of 5.15 pch. Its average performance was also more stable across runs. These results confirm its capability to explore the Pareto front; however, the observed variability suggests that additional mechanisms may be required to refine workload balancing on complex real–world instances.

HMOSA achieved the lowest values across both distance and workload objectives, with a best of 1,346.85 km. and a consistently low load SD of 1.65 pch. in both the best and average cases. This demonstrates the effectiveness of integrating warm–start initialization, archive–based selection, and a guided neighborhood search, allowing the algorithm to explore promising regions of the solution space while preserving stability across runs.

In addition to aggregated performance results, the comparison retains the best distance and best load standard deviation for each method. These values are not intended to imply overall superiority but to highlight extreme solutions that support managerial decisions. In practical routing operations, especially in the school milk context, planners often review the minimum–distance case and the most balanced–workload case before choosing a compromise that matches operational priorities. Presenting these extremes helps visualize the trade–off frontier and allows stakeholders to assess how fairness improvements may require additional travel distance. Thus, including best values acts as a decision–support feature, aligning with the objective of using HMOSA for real–world planning.

To evaluate the quality of the obtained Pareto solutions, two widely adopted metrics were used: Inverted Generational Distance (IGD) and Hypervolume (HV). IGD measures how close the obtained solutions are to the true Pareto front, where smaller values indicate stronger convergence, while HV quantifies the extent of the dominated objective space and reflects solution diversity. These indicators have been commonly employed in recent multi–objective VRP studies and are considered essential for assessing both convergence reliability and Pareto–front coverage [25–26]. As shown in **Table 5**, HMOSA achieved the lowest IGD and the highest HV values across all problem sizes, demonstrating consistent dominance in both convergence and solution diversity while preserving well–distributed trade–off solutions. As the problem size increased, this trend became more evident. For example, the IGD value of HMOSA decreased from 0.0997 in the 10–customer case to 0.0286 in the intermediate 30–customer case and remained comparatively low at 0.0531 in the real–world instance of 51 customers. In contrast, both MOSA and NSGA–II reported considerably higher IGD values across all scales.

HMOSA also yielded the highest HV values in all cases, reaching 1.1524 and 1.0866 for the 30– and 51–customer instances, which confirms that the algorithm consistently explored more promising regions of the objective space than MOSA and NSGA–II.

These results demonstrate that HMOSA provides not only superior objective values but also strong convergence behavior and Pareto set diversity when the problem scale increases. This characteristic is important for practical routing applications where reliable performance is required across different operational environments. Overall, the findings confirm that the hybrid structure of HMOSA supports algorithmic robustness and practical scalability for real distribution planning.

Table 5 Comparison of IGD and HV results for MOSA, NSGA–II and HMOSA at different scales

No. of customers	MOSA		NSGA–II		HMOSA	
	IGD	HV	IGD	HV	IGD	HV
10	0.1069	1.1171	0.1461	0.6494	0.0997	1.1163
30	0.1506	0.9579	0.0706	1.0856	0.0286	1.1524
51	0.2894	0.6488	0.1462	1.0052	0.0531	1.0866

Figure 3 further illustrates the Pareto fronts obtained from MOSA and HMOSA. The Pareto front of MOSA appears widely scattered and biased toward solutions with longer distances and higher workload variability. In contrast, HMOSA produced a more compact and well–defined Pareto front that lies closer to the efficient frontier, demonstrating that it simultaneously improved both objectives. Importantly, HMOSA's solutions clustered in the lower–left region of the graph, which represents desirable combinations of shorter travel distances and balanced vehicle loads.

In addition, NSGA–II was also tested to provide a complementary reference from a population–based approach. Its Pareto front showed a wider exploratory spread, which indicates a strong search capability, yet the solutions tended to be more dispersed and demonstrated higher variability in load balance. When compared visually, HMOSA maintained a clearer trend toward the efficient region, especially in the lower–left portion of the objective space, suggesting that its guided neighborhood strategy helped preserve both convergence and practicality in the trade–off solutions.

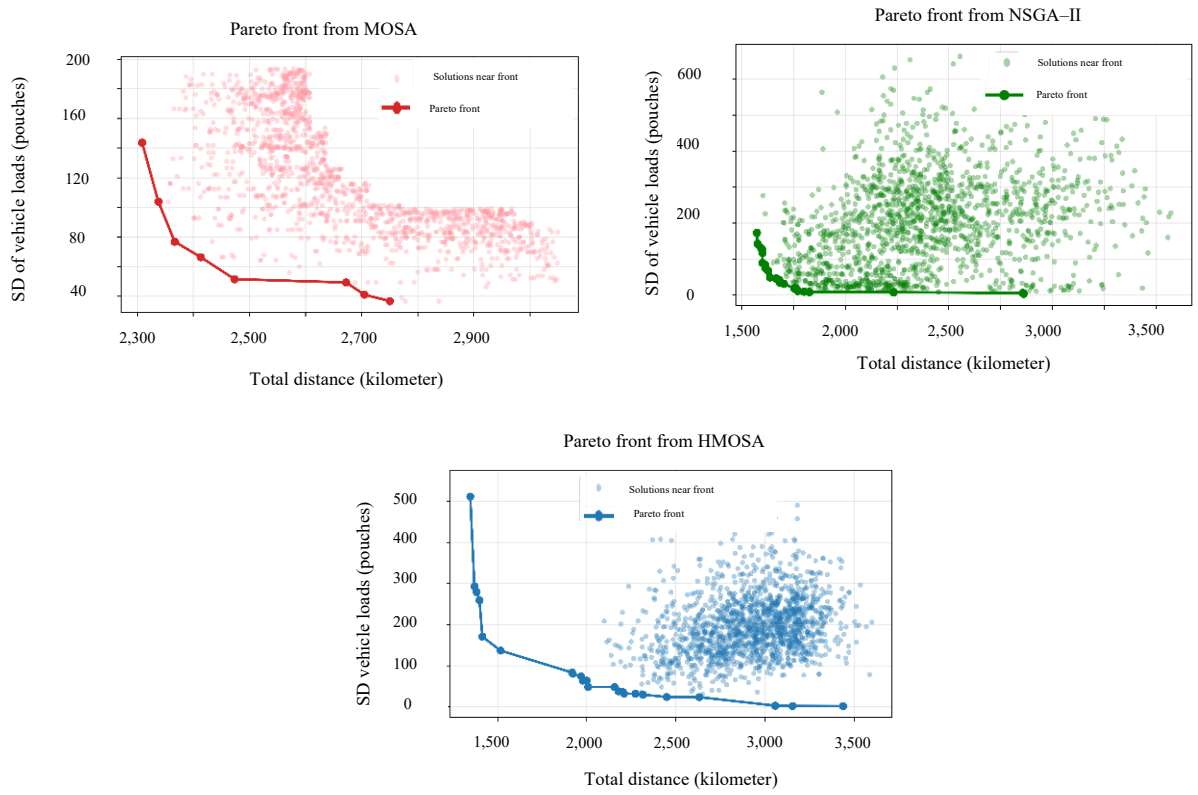

Figure 3 Pareto front from MOSA, NSGA–II and HMOSA

5.2 Sensitivity Analysis of Algorithm Parameters

To further investigate the behavior of the proposed HMOSA algorithm and to assess its robustness under different parameter settings, a one–factor–at–a–time (OFAT) sensitivity analysis was conducted. The baseline configuration was first calibrated through preliminary experiments and adopted as the default setting for the HMOSA algorithm in the main study. The purpose of the sensitivity analysis was therefore not to replace the baseline, but to investigate how each parameter individually influences the algorithm's behavior and to identify potential alternatives that might be beneficial under different operational requirements. After this primary comparison, seven configurations (S0–S6) were designed to examine the influence of individual parameters on search performance, while only one parameter was adjusted at a time and all the others were held constant. The full parameter settings adopted in this experiment are presented in **Table 6**.

Table 6 Parameter settings for the HMOSA sensitivity analysis on the 51–customer case

scenario	T_0	T_{min}	Cooling rate	$p_{accept\_nondominated}$
S0	500	10^{-3}	0.995	0.90
S1	400	10^{-3}	0.995	0.90
S2	600	10^{-3}	0.995	0.90
S3	500	10^{-3}	0.985	0.90
S4	500	10^{-3}	0.999	0.90
S5	500	10^{-3}	0.995	0.70
S6	500	10^{-3}	0.995	0.95

In this analysis, three parameters were selected for examination: the initial temperature (T_0), the cooling rate, and the acceptance probability for non–dominated solutions ($p_{\text{accept\_nondominated}}$). These parameters were chosen because they directly influence the degree of exploration, convergence behavior, and diversity of the Pareto front. Scenarios S1 and S2 varied only the initial temperature to test the effect of faster convergence (S1) or increased randomness at the start of the process (S2). Scenarios S3 and S4 modified the cooling rate, which is known to be highly sensitive in simulated annealing–based approaches, to analyze whether broader exploration (S3) or prolonged diversification (S4) could influence computational cost and solution quality. Finally, Scenarios S5 and S6 focused on adjusting the acceptance probability for non–dominated solutions to explore how different levels of diversification and exploitation affect the overall performance.

After running all seven scenarios using the same dataset and stopping criteria, the results were summarized in **Table 7**, which reports the best achieved distance, load standard deviation, hypervolume (HV), IGD, and computational time (in seconds) for each configuration.

Table 7 HV and IGD values for HMOSA under different parameter settings (51–customer case)

scenario	Best Distance (km.)	Best Load SD (pch.)	HV	IGD	Time (sec)
S0	1,346.85	1.65	0.0369	1.0864	21.03
S1	1,346.98	1.87	0.0457	1.0637	20.76
S2	1,368.35	1.57	0.0643	1.1029	21.52
S3	1,391.09	2.06	0.0884	1.0688	7.82
S4	1,360.13	0.70	0.0639	1.0601	104.95
S5	1,358.41	1.58	0.0560	1.0891	21.70
S6	1,358.38	2.28	0.0616	1.0670	22.46

Table 7 shows that varying the parameter settings around the calibrated baseline (S0) did not lead to any severe performance degradation, indicating that the proposed HMOSA algorithm exhibits a reasonable degree of robustness. Across all scenarios, the best distance, load standard deviation, HV, and IGD values remain within a relatively narrow range, and the computational times are also stable, except for the intentionally extreme setting in S4. The baseline configuration (S0) continues to provide one of the best travel distances with a balanced load standard deviation and a moderate runtime, which reflects a conservative convergence towards a high–quality region in the objective space. This conservative yet reliable behavior is the main reason why S0 was adopted as the default parameter setting in the main experiments.

The alternative scenarios mainly illustrate how small perturbations in the parameters shift the balance between convergence quality, Pareto–front diversity, and computational effort. For example, S1 slightly improves IGD and HV relative to S0, but the gains are modest and accompanied by a small increase in load variability. S2 and S5 achieve somewhat higher HV values than S0 but at the cost of worse IGD, suggesting that a wider Pareto front does not always translate into better proximity to the reference set. S3 yields the highest HV and the shortest runtime, showing that a more exploratory cooling schedule can generate a more diverse set of solutions efficiently; however, this comes with noticeably higher total distance and load imbalance, which may be less desirable in practice. Conversely, S4 produces the lowest IGD and an excellent load standard deviation, together with a reasonably high HV value, but requires a much longer computational time, limiting its suitability for time–sensitive applications. Scenario S6 also illustrates a more exploratory behavior, with improved HV compared with S0 but again at the price of poorer load balancing.

Overall, these results confirm that HMOSA maintains stable and acceptable performance under controlled parameter variation, supporting the robustness of the proposed framework. The differences between S0 and the alternative configurations are relatively small in most metrics, and no scenario leads to a collapse in solution quality. In this context, S0 remains a suitable

default choice when a balanced and dependable performance is required, while configurations such as S3 or S4 may be considered in situations where either a wider Pareto front or slightly better convergence is desired and additional computational effort is acceptable. The observed trade–offs therefore provide useful guidance for practical parameter tuning and reinforce the reliability and flexibility of the HMOSA algorithm for real–world applications.

5.3 Managerial Interpretation and Decision–Support Insights

From a managerial perspective, this graphical representation is highly informative. The Pareto front reveals the inherent trade–off between minimizing distance and achieving workload balance. For instance, solutions on the extreme distance–minimizing side reduce total travel distance but result in uneven load distribution across vehicles, placing disproportionate burden on certain delivery teams. Conversely, solutions on the load–balancing extreme provide equitable workloads but require slightly longer travel distances. The compromise solutions generated by HMOSA highlight practical compromises, where moderate increases in distance can substantially improve workload equity, offering decision–makers viable trade–offs between distance and fairness.

In the context of Thailand's School Milk Program, these trade–offs are not merely theoretical. Distribution activities involve not only transportation but also manual unloading of pouches at each school, which means that workload imbalance translates directly into physical strain and fatigue for some delivery teams. If one vehicle is assigned disproportionately high demand, its driver–assistant pair must spend substantially more time and effort compared to others, even if the overall distance is minimized. Conversely, evenly distributed workloads can enhance equity and morale among staff but often require longer travel distances. To illustrate these practical implications more clearly, three representative Pareto solutions were selected and analyzed at the vehicle level, as summarized in **Table 8**. These examples highlight how different routing strategies affect both total distance and workload allocation across the fleet, providing concrete evidence of the operational consequences behind abstract performance indicators.

Table 8 Comparison of Distance and Load Across Selected Pareto Solutions

vehicle	Distance (kilometer)/Load of each pareto solution (pouches)		
	Pareto_01 (Min Distance)	**Pareto_45 (Compromise)**	**Pareto_91 (Min SD)**
1	128.7 / 2,945	693.3 / 3,184	729.2 / 3,143
2	101.8 / 3,427	187.0 / 3,247	433.3 / 3,145
3	65.5 / 1,860	272.9 / 3,132	275.7 / 3,145
4	74.0 / 3,262	157.2 / 2,983	702.8 / 3,148
5	584.7 / 3,417	192.7 / 3,070	255.6 / 3,142
6	98.7 / 3,483	136.5 / 3,226	220.6 / 3,145
7	157.4 / 3,317	126.6 / 3,109	197.6 / 3,144
8	136.0 / 3,446	151.4 / 3,206	624.1 / 3,145

Table 8 illustrates the vehicle–level results for three representative Pareto solutions: the minimum–distance solution (Pareto_01), a compromise solution (Pareto_45), and the minimum–imbalance solution (Pareto_91). In Pareto_01, the total distance is minimized at 1,346.9 km., representing the minimum distance routing plan in terms of fuel consumption and travel time. However, the workload imbalance is extreme: Vehicle 3 carries only 1,860 pch., while Vehicle 6 carries as much as 3,483 pch., a disparity of more than 1,600 pch. Such uneven distribution implies that certain delivery teams face nearly double the workload of others. Although this solution reduces total travel distance, it risks overburdening specific teams, which may lead to fatigue, slower service, and lower workforce satisfaction.

At the opposite extreme, Pareto_91 achieves almost perfect workload balance, with every vehicle carrying approximately 3,140–3,148 pch. The standard deviation of load drops to only 1.65, meaning that no team bears a disproportionately higher burden. Yet, this comes at the expense of a very high total distance of 3,438.8 km, which is more than 2,000 km longer than the minimum–distance case. While this solution ensures fairness and equity across delivery teams, the additional travel would substantially increase fuel consumption and total travel distance, which directly translates into higher operating cost, as well as environmental impact, making it less practical under real–world budgetary constraints.

A more pragmatic option is Pareto_45, the compromise solution, where the total distance is 1,917.7 km., higher than Pareto_01 but still substantially lower than Pareto_91. In this case, the workload disparity is reduced significantly: the lightest–loaded vehicle (Vehicle 4 with 2,983 pch.) differs from the heaviest (Vehicle 2 with 3,247 pch.) by only 264 pch.. All other vehicles fall within a narrow range around 3,000 pch., providing a far more equitable distribution of workload while keeping travel distance at a manageable level. This solution exemplifies the strength of HMOSA in identifying balanced trade–offs: modest additional distance secures substantial gains in fairness without the excessive cost of the fully balanced solution.

In practice, managers should not only view the Pareto solutions as abstract trade–offs but also integrate them into operational policies. Fairness can

be introduced as a managerial guideline, for example by monitoring the deviation in vehicle loads and keeping it within an acceptable range. Compromise solutions such as Pareto_45 can serve as baseline routing plans, which can be periodically updated when school demands fluctuate, ensuring that both efficiency and equity are maintained over time. Adopting balanced workloads reduces the hidden costs of worker fatigue, absenteeism, and turnover, thereby supporting the long–term sustainability of the program. Finally, the proposed HMOSA approach can be embedded into decision–support tools for regional contractors and policy makers, enabling them to compare scenarios and select routing strategies that best align with organizational priorities, budget constraints, and workforce well–being.

6. Conclusion

This study proposed a Hybrid Multi–Objective Simulated Annealing (HMOSA) framework for the school milk routing problem in Thailand, where workload distribution is directly linked to manual unloading tasks. By jointly minimizing total travel distance and balancing vehicle workloads, the proposed approach explicitly captures the trade-off between operational efficiency and labor fairness. Unlike studies that approximate workload from service time, the present formulation captures physical effort through the standard deviation of vehicle loads. This aligns with recent research on workload–balancing vehicle routing problem and offers a more interpretable fairness indicator for labor–intensive logistics settings. The results showed that HMOSA outperformed SA and MOSA and achieved superior Pareto–front performance compared with NSGA–II. The structured warm–start strategy and guided neighborhood mechanism enhanced convergence and solution diversity and were validated using HV and IGD metrics. These findings extend current knowledge by demonstrating that trajectory–based heuristics can remain effective when both distance efficiency and fairness are considered in operational decision–making.

Several limitations exist. The model uses only two objectives, relies on data from a single contractor, and does not incorporate driver fatigue. Future work may integrate additional operational constraints or multi–period planning. Overall, HMOSA provides a practical and scalable decision–support framework that connects multi–objective optimization research with real routing applications.

7. References

[1] Z. H. Ahmed, N. Al-Otaibi, A. Al-Tameem and A. K. J. Saudagar, "Genetic Crossover Operators for the Capacitated Vehicle Routing Problem," *Computers, Materials & Continua*, vol. 74, no. 1, pp. 1575–1605, 2023, doi: 10.32604/cmc.2023.031325.

[2] C. Wang, B. Ma and J. Sun, "A co-evolutionary genetic algorithm with knowledge transfer for multi-objective capacitated vehicle routing problems," *Applied Soft Computing*, vol. 148, 2023, Art. no. 110913, doi: 10.1016/j.asoc.2023.110913.

[3] M. Kumari, P. K. De, K. Chaudhuri and P. Narang, "Utilizing a hybrid metaheuristic algorithm to solve capacitated vehicle routing problem," *Results in Control and Optimization*, vol. 13, 2023, Art. no. 100292, doi: 10.1016/j.rico.2023.100292.

[4] J. Li, R. Liu and R. Wang, "Handling dynamic capacitated vehicle routing problems based on adaptive genetic algorithm with elastic strategy," *Swarm and Evolutionary Computation*, vol. 86, 2024, Art. no. 101529, doi: 10.1016/j.swevo.2024.101529.

[5] X. Zhang, Y. Hao, L. Zhang and X. Yuan, "Application of improved genetic algorithm to vehicle routing problem considering the environmental self-regulation of the freight companies," *Expert Systems with Applications*, vol. 274, 2025, Art. no. 127010, doi: 10.1016/j.eswa.2025.127010.

[6] R. Kuo, M. Luthfiansyah, N. Masruroh and F. E. Zulvia, "Application of improved multi-objective particle swarm optimization algorithm to solve disruption for the two-stage vehicle routing problem with time windows," *Expert Systems with Applications*, vol. 225, 2023, Art. no. 120009, doi: 10.1016/j.eswa.2023.120009.

[7] A. Thammano and P. Rungwachira, "Hybrid modified ant system with sweep algorithm and path relinking for the capacitated vehicle routing problem," *Heliyon*, vol. 7, no. 9, 2021, Art. no. e08029, doi: 10.1016/j.heliyon.2021.e08029.

[8] A. Motaghedi-Larijani, "Solving the number of cross-dock open doors optimization problem by combination of NSGA-II and multi-objective simulated annealing," *Applied Soft Computing*, vol. 128, 2022, Art. no. 109448, doi: 10.1016/j.asoc.2022.109448.

[9] V. F. Yu, S.-W. Lin, L. Zhou and R. Baldacci, "A fast simulated annealing heuristic for the multi-depot two-echelon vehicle routing problem with delivery options," *Transportation Letters*, vol. 16, no. 8, pp. 921–932, 2023, doi: 10.1080/19427867.2023.2257923.

[10] E. Rodríguez-Esparza, A. D. Masegosa, D. Oliva and E. Onieva, "A new Hyper-heuristic based on Adaptive Simulated Annealing and Reinforcement Learning for the Capacitated Electric Vehicle Routing Problem," *Expert Systems with Applications*, vol. 252, 2024, Art. no. 124197, doi: 10.1016/j.eswa.2024.124197.

[11] T. Leelertkij, J. Buddhakulsomsiri and V. -N. Huynh, "A multi-thread simulated annealing for multi-objective vehicle routing problem with time windows and demand priority," *Computers & Industrial Engineering*, vol. 207, 2025, Art. no. 111253, doi: 10.1016/j.cie.2025.111253.

[12] V. Praveen, P. Keerthika, G. Sivapriya, A. Sarankumar and B. Bhasker, "Vehicle Routing Optimization Problem: A Study on Capacitated Vehicle Routing Problem," *Materials Today: Proceedings*, vol. 64, pp. 670–674, 2022, doi: 10.1016/j.matpr.2022.05.185.

[13] Z. Nan, X. Yang, L. Ruiz-Garcia, J. Qiu, Y. Feng and J. Han, "Multi-objective optimization of cold chain distribution routes considering traffic congestion," *Agriculture Communications*, vol. 3, no. 4, 2025, Art. no. 100104, doi: 10.1016/j.agrcom.2025.100104.

[14] S. I. Nyako, D. Tayachi and F. Abdelaziz, "Machine learning multi-objective optimization for time-dependent green vehicle routing problem," *Energy Economics*, vol. 148, 2025, Art. no. 108628, doi: 10.1016/j.eneco.2025.108628.

[15] M. Vukićević, M. Ratli, A. Rivenq, R. Todosijević and B. Jarboui, "Energy minimizing capacitated covering vehicle routing problem," *Applied Soft Computing*, vol. 183, 2025, Art. no. 113620, doi: 10.1016/j.asoc.2025.113620.

[16] Z. Wu and H. Yaman, "Comparison of compact formulations for the electric vehicle routing problem," *Transportation Research Part B: Methodological*, vol. 200, 2025, Art. no. 103314, doi: 10.1016/j.trb.2025.103314.

[17] H. Yu and W. D. Solvang, "Incorporating flexible capacity in the planning of a multi-product multi-echelon sustainable reverse logistics network under uncertainty," *Journal of Cleaner Production*, vol. 198, pp. 285–303, 2018, doi: 10.1016/j.jclepro.2018.07.019.

[18] Z. Yanhu, Y. Lijuan, K. ShuMei and M. Decheng, "Research on multi-objective optimization of multi-endpoint VRP with time window for the distribution of seasonal products by multi-homing heterogeneous fleets," *Expert Systems with Applications*, vol. 298, 2026, Art. no. 129595, doi: 10.1016/j.eswa.2025.129595.

[19] P. Matl, R.F. Hartl and T. Vidal, "Workload equity in vehicle routing: The impact of alternative workload resources," *Computers and Operations Research*, vol. 110, pp. 116–129, 2019. doi: 10.1016/j.cor.2019.05.016.

[20] F. Lehuédé, O. Péton and F. Tricoire, "A lexicographic minimax approach to the vehicle routing problem with route balancing," *European Journal of Operational Research*, vol. 282, no. 1, pp. 129–147, 2020, doi: 10.1016/j.ejor.2019.09.010.

[21] S. Shahnejat-Bushehri, A. Kermani, O. Arslan, J.-F. Cordeau and R. Jans, "A Vehicle Routing Problem with Time Windows and Workload Balancing for COVID-19 Testers: A case study," *IFAC-PapersOnLine*, vol. 55, no. 10, pp. 2920–2925, 2022, doi: 10.1016/j.ifacol.2022.10.175.

[22] J. Li, Y. Fang and N. Tang, "A cluster-based optimization framework for vehicle routing problem with workload balance," C*omputers & Industrial Engineering*, vol. 169, 2022, Art. no. 108221, doi: 10.1016/j.cie.2022.108221.

[23] W. Zhao, Y. Yuan, C. Cheng and W. Liu, "Bi-objective sustainable urban logistics vehicle routing problem with workload balance," *Journal of Industrial Information Integration*, vol. 48, 2025, Art. no. 100985. doi: 10.1016/j.jii.2025.100985.

[24] X. Xu and H. Ouyang, "A branch-and-cut algorithm for the pallet-loading vehicle routing problem considering load balance of semi-trailer trucks," *Computers & Operations Research*, vol. 185, 2025, Art. no. 107258, doi: 10.1016/j.cor.2025.107258.

[25] J. Wang, Y. Zhou, Y. Wang, J. Zhang, C. L. P. Chen and Z. Zheng, "Multiobjective Vehicle Routing Problems With Simultaneous Delivery and Pickup and Time Windows: Formulation, Instances, and Algorithms," *IEEE Transactions on Cybernetics*, vol. 46, no. 3, pp. 582–598, 2016, doi: 10.1109/TCYB.2015.2409837.

[26] J. Wang, T. Weng and Q. Zhang, "A Two-Stage Multiobjective Evolutionary Algorithm for Multiobjective Multidepot Vehicle Routing Problem With Time Windows," *IEEE Transactions on Cybernetics*, vol. 49, no. 7, pp. 2467–2478, 2019, doi: 10.1109/tcyb.2018.2821180